International Journal of Nanomedicine

Dovepress
open access to scientific and medical research

Open Access Full Text Article

ORIGINAL RESEARCH

Influence of Acidic Environment on Hydrolytic Stability of MDP-Ca Salts with Nanolayered and Amorphous Structures

Qing Zhao[1,*], Yixue Gao[2,*], Xin Jin[1], Fei Han[2], Kai Chen[3], Chen Chen[1]

[1]Department of Endodontics, The Affiliated Stomatological Hospital of Nanjing Medical University, Jiangsu Province Key Laboratory of Oral Diseases, Jiangsu Province Engineering Research Center of Stomatological Translational Medicine, Nanjing, 210029, People's Republic of China; [2]Department of Prosthodontics, The Affiliated Stomatological Hospital of Nanjing Medical University, Jiangsu Province Key Laboratory of Oral Diseases, Jiangsu Province Engineering Research Center of Stomatological Translational Medicine, Nanjing, 210029, People's Republic of China; [3]Collaborative Innovation Center of Atmospheric Environment and Equipment Technology, Jiangsu Key Laboratory of Atmospheric Environment Monitoring and Pollution Control, School of Environmental Science and Engineering, Nanjing University of Information Science and Technology, Nanjing, 210044, People's Republic of China

*These authors contributed equally to this work

Correspondence: Chen Chen, Department of Endodontics, The Affiliated Stomatological Hospital of Nanjing Medical University, Jiangsu Province Key Laboratory of Oral Diseases, Jiangsu Province Engineering Research Center of Stomatological Translational Medicine, Nanjing, 210029, People's Republic of China, Tel +8625 6959 3031, Fax +8625 8651 6414, Email ccchicy@njmu.edu.cn

Purpose: This study aimed to investigate the hydrolytic stability of 10-methacryloyloxydecyl dihydrogen phosphate calcium (MDP-Ca) salts with nanolayered and amorphous structures in different pH environments.

Methods: The MDP-Ca salts were synthesized from MDP and calcium chloride and characterized by X-ray diffraction (XRD), nuclear magnetic resonance (NMR), and transmission electron microscopy (TEM). Inductively coupled plasma-mass spectrometry (ICP-MS) was used to quantify the release of calcium from the synthesized MDP-Ca salt, MDP-treated hydroxyapatite (MDP-HAp), and untreated HAp after soaking in acidic and neutral solutions for 1, 7, and 30 days. To study the hydrolytic process, we carried out molecular dynamics (MD) simulations of the nanolayered MCS-MD (monocalcium salt of the MDP dimer) and DCS-MD (dicalcium salt of the MDP dimer) structures, as well as of the amorphous-phase MCS-MM (monocalcium salt of the MDP monomer).

Results: The TEM images showed that the nanolayered structures were partially degraded by acid attack. Based on the ICP-MS results, the hydrolysis rate of the MDP-Ca salt in acidic and neutral environments followed the order HAp > MDP-HAp > MDP-Ca salt. The MD simulations showed that, in acidic environments, clusters of MDP remained aggregated and all Ca^{2+} ions separated from the MDP monomer to interact with water molecules in aqueous solution. In neutral environments, Ca^{2+} ions always interacted with phosphate groups, OH^- ions, and water molecules to form clusters centered on Ca^{2+} ions.

Conclusion: MDP-Ca presented higher hydrolysis rates in acidic than neutral environments. Nanolayered MCS-MD possessed the highest resistance to acidic hydrolysis, followed by amorphous MCS-MM and DCS-MD.

Keywords: 10-methacryloyloxydecyl dihydrogen phosphate calcium salts, nanolayering, hydrolysis, molecular dynamics simulations, dentin bonding

Introduction

Resin filling and resin luting cement-based restorations lose their marginal seal after clinical service, due to nanoleakage and degradation at the adhesive interface;[1–3] this induces marginal discoloration or secondary caries,[4,5] finally impairing the clinical performance.[1] Furthermore, every restoration replacement inevitably weakens the tooth and leads to increased medical costs.[6–8] Therefore, improving the durability of the dentin–resin bonding interface have been actively pursued. In 1982, Nakabayashi first proposed that the formation of a hybrid layer is the key to dentin bonding.[9] Preventing the

Received: 24 January 2022
Accepted: 5 April 2022
Published: 13 April 2022

Graphical Abstract

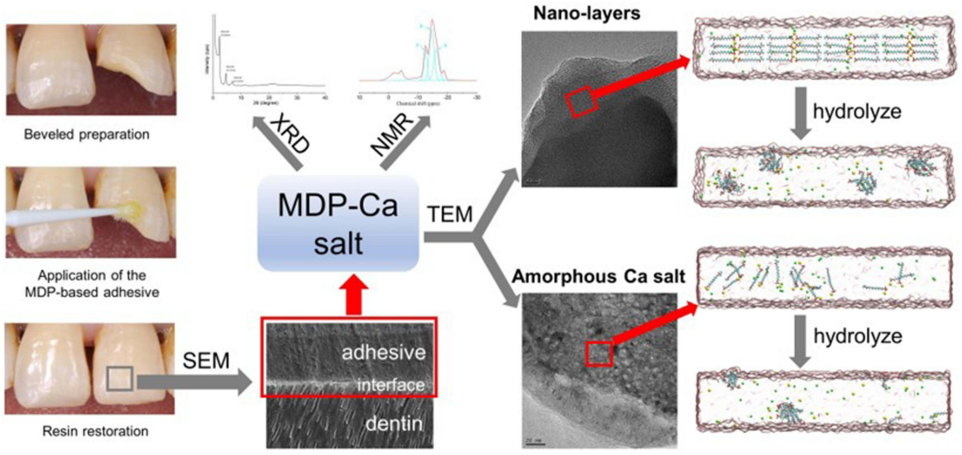

degradation of the hybrid layer [composed of demineralized collagen, resin, residual water, and hydroxyapatite (HAp) crystallites] is currently considered one of the most effective ways to improve the dentin bond durability.[10]

Confirming the validity of the hybrid layer theory took more than twenty years. During this period, a phosphate monomer, 10-methacryloyloxydecyl dihydrogen phosphate (MDP), has gradually become the core functional component of typical dentin bonding agents.[9] This is not only because of the expired patent protection for MDP, but also owing to the evidence for the demineralization ability of MDP and its chemical affinity to HAp.[11,12] It has been reported that MDP can form calcium salts with HAp exhibiting the lowest dissolution rate among almost all adhesion-promoting monomers.[9,11,13] The advantage of this characteristic is that the less soluble the calcium salt is, the stronger and more stable its adhesion to HAp, which improves the stability of the ultrastructure of the adhesive interface and the bond durability.[14,15]

The self-assembled, ordered, and nanolayered structure of interconnected MDP-Ca salts at the adhesive interface was another surprising discovery highlighting the superiority of MDP.[16] Some studies have reported that the nanolayered structure at the interface can extend from the hybrid to the adhesive resin layer, resulting in a tighter connection between the two layers. The authors of these studies concluded that the nanolayered structure possessed a higher elastic modulus than the surrounding adhesive resin, and their 3D continuous structures contributed to the mechanical strengthening of the adhesives in the same way as filler particles.[17] Each nanolayer of the self-assembled MDP structure consists of two MDP molecules oriented with their methacrylate groups directed toward each other and their functional hydrogen phosphate groups directed away from each other; each phosphate group of MDP is bridged to the adjacent group by a Ca ion.[18] The strong hydrophobicity of the nanolayered 10-carbon chains contributes to eliminate residual water surrounding the nanolayer, protecting collagen fibrils from water-induced degradation in the local microenvironment of the hybrid layer.[14,19] The demineralized residual apatite crystals in the hybrid layer react with MDP to form a dense nanolayered structure that is resistant to acid degradation.[16] The properties of the nanolayered structure discussed above support the transition from an inorganic substrate to an artificial biomaterial of organic nature,[16] which could be responsible for the remarkable in vivo and in vitro dentin bonding performances of MDP-based adhesives.[14,20,21]

Nevertheless, there is no evidence showing that the MDP-Ca salt necessarily form a nanolayered structure. The molecular components of MDP-Ca salts that form a layered structure were determined to be the monocalcium and dicalcium salts of the MDP dimer (MCS-MD and DCS-MD, respectively). However, the monocalcium salt of the MDP monomer (MCS-MM) predominantly produced by dentin does not contribute to the formation of the nanolayered structure. Instead, MCS-MD can form a tightly-packed amorphous phase via hydrogen bond interactions.[22]

Nanolayers could be detected even after 9 years of clinical service at the interface of a restoration applied using a commercial MDP-based adhesives.[17] An in vitro study confirmed that MDP-Ca salt was almost insoluble in neutral water in one year.[11] Unfortunately, a recent in vitro investigation showed that the nanolayers formed by MDP and amorphous calcium phosphate were partially degraded or even severely damaged after acidic (pH = 5) and alkaline (pH = 10) attacks.[23] In the complex oral environment, cariogenic bacteria such as *Streptococcus mutans* and *Lactobacillus* can produce acids during metabolization, leading to a low cariogenic pH range of 4.5–5.5, or even below 4.2 after loss of the marginal seal of the restoration.[24,25] Furthermore, frequent consumption of acidic beverages or similar habits could lead to abnormal demineralization of the tooth surface and caries,[26] or even worse consequences at the complete dentin–adhesive interface. Therefore, an important question is whether a low pH would induce unpredictable hydrolysis of MDP-Ca salts in the hybrid layer. Another issue that should be investigated is whether the MDP-Ca salts in other structures besides of nanolayered one could remain stable in an acidic environment. This is a critical requirement for the appropriate evaluation of the dentin-bonding performance of MDP-based adhesives.

In this study, we synthesized and characterized MDP-Ca salts with nanolayered and amorphous structures; then, we measured the hydrolytic degradation rates of both structures upon soaking in different pH solutions. The stabilities of different MDP-Ca salts in acidic and neutral environments were studied by molecular dynamics (MD) simulations, with the aim to evaluate the effect of the acidic environment on the ionic bonding in MDP-Ca salts with nanolayered and amorphous structures. The hypotheses tested were that: (i) the hydrolytic degradation rate of MDP-Ca salts in both structures are affected by the pH of the environment and (ii) the MDP-Ca salt with nanolayered structure provides higher resistance to acid degradation than that with amorphous structure.

Materials and Methods

Synthesis and Characterization of MDP-Ca Salt

$CaCl_2$ (0.003 mol, Macklin, China) was stirred in 5 mL of 50 vol.% aqueous ethanol solution, and MDP (0.003 mol, Watson International Ltd., China) was dissolved into 5 mL of ethanol solution. Afterward, the MDP solution was added to the $CaCl_2$ solution under vigorous stirring. After 12 h at room temperature, the reactant was centrifuged and the supernatant was discarded. The reactant was washed three times with absolute ethanol and distilled water in sequence to remove unreacted MDP and $CaCl_2$, and then dried in air at room temperature for 48 h. X-ray diffraction (XRD) and nuclear magnetic resonance (NMR) were then used to examine the reactant.

The crystal phase of the reactant was identified by XRD (D8 Advance, Bruker, Germany) at an acceleration voltage of 40 kV, a current of 200 mA, and a scanning rate of 0.02° s^{-1} for $2\theta/\theta$ scans. The ^{31}P NMR spectrum of the reactant was measured using an AVANCE III HD 400M (Bruker, Germany) spectrometer with ammonium dihydrogen phosphate as the external reference. The spectra were analyzed using the Mestrenova and OriginPro 8.0 Data Analysis and Graphing Software (OriginLab Co., USA).

Transmission Electron Microscopy (TEM) Measurements

The reactant was submerged in acetic acid aqueous solution (pH ≈ 4) and deionized water (pH ≈ 7) for 15 min. Then, the resulting solutions were further washed three times with distilled water. The obtained samples were ultrasonically dispersed with absolute ethanol for 30 min. One-microliter droplets of suspension were then deposited on a holey carbon film before observation. After drying at room temperature, the samples were observed using a high-resolution transmission electron microscope (Tecnai G2 20, FEI, Czech Republic) equipped with the Gatan Digital Micrograph software at a 200 keV accelerating voltage.

Inductively Coupled Plasma-Mass Spectrometry (ICP-MS)

A 0.2 g amount of HAp powder (Sigma Chemical Co., USA) was treated with 2.0 g of MDP-containing primer (10 wt.% MDP, 40 wt.% ethanol, and 40 wt.% water) for 12 h. The treated HAp powder sample was washed in ethanol, centrifuged three times, and dried in air for 48 h at room temperature.

Each of the synthesized MDP-Ca salt, HAp/MDP mixture, and HAp was submerged in 3 mL of 37 °C acetic acid aqueous solution (pH = 4) or deionized water (pH ≈ 7). After soaking for 1, 7, and 30 days, the calcium content of the soaking liquids from each group was determined by ICP-MS (ICAP-QC, Thermo Scientific, USA).

MD Simulations

All MD simulations were carried out using the Gromacs 2021.2 software;[27] geometry optimization of the MDP molecule was performed using the Gaussian 16 package.[28] The MDP molecule was optimized using the B3LYP exchange–correlation functional with the 6-31G (d,p) basis set for all atoms. Partial atomic charges were then calculated by the restrained electrostatic potential (RESP) method at the B3LYP/6-31G(d,p) level.[29] The MDP molecules were described using the general AMBER Force Field (GAFF) field parameters,[30] while the the TIP3P model was used to represent water molecules. The simulated temperature was adjusted to 300 K, and the simulations were carried out in the isothermal–isobaric (NPT) ensemble with cubic periodic boundary conditions. The time step of the MD simulations was 1 fs. The particle-mesh Ewald (PME) approach was used to model long-range electrostatic interactions,[31] and the van der Waals interaction radius was set to 1.2 nm. The chlorine counter ions were then added to the solvated box to neutralize it.

In two separate models, MCS-MD and DCS-MD self-assembled into nanolayered structures. The MCS-MM model consisted of an amorphous phase that was randomly placed in rectangular water boxes.

Results

Characterization

Figure 1A shows the XRD pattern of synthesized MDP-Ca salts. Three characteristic peaks (2θ = 2.32°, 4.62°, 6.94°) reflect the nanolayered structure of MDP-Ca salts. The *d*-spacing calculated from the peak with the strongest signal (2θ = 2.32°) was 3.84 nm. Figures 1B–D show the typical ^{31}P NMR spectrum of synthesized MDP-Ca salts, a partially

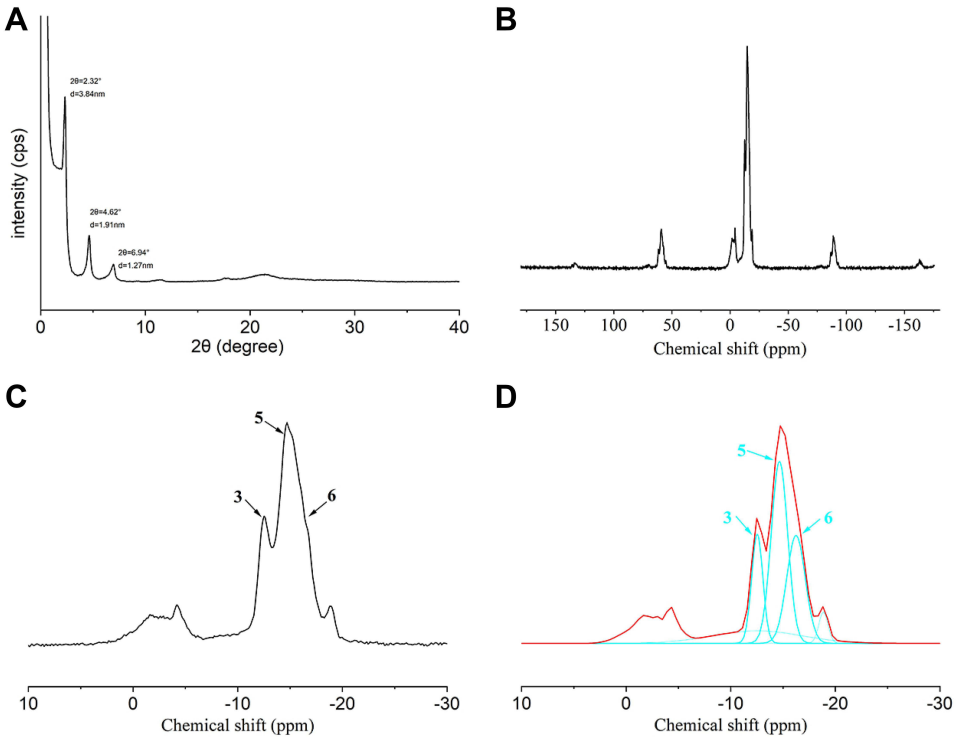

Figure 1 XRD pattern and NMR spectra of synthesized MDP-Ca salts. (**A**) XRD pattern of synthesized MDP-Ca salts. (**B**) Typical ^{31}P NMR spectrum of synthesized MDP-Ca salts. (**C**) Partially enlarged view of the NMR spectrum. The arrows mark the NMR peaks assigned to the phosphorus atoms of the MDP-Ca salts; the corresponding assignments of the numbered peaks are shown in Table 1. (**D**) Curve-fitting results corresponding to the observed ^{31}P NMR spectrum of synthesized MDP-Ca salts. The sky-blue lines correspond to the simulated peaks 3, 5, and 6 for the three MDP-Ca salts. The red line is the resulting overall spectrum.

Table 1 Chemical Structures of Three Detected Types of MDP-Ca Salt

Peak Label	MDP-Ca-Salt	Chemical Structure
3	Di-calcium salt of the MDP dimer (DCS-MD)	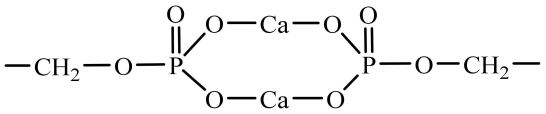
5	Mono-calcium salt of the MDP monomer (MCS-MM)	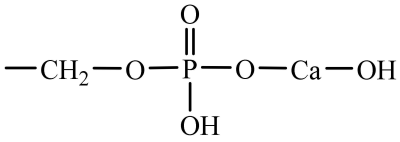
6	Mono-calcium salt of the MDP dimer (MCS-MD)	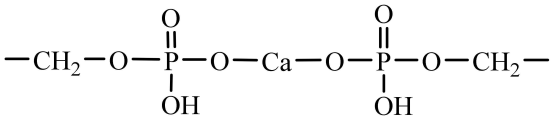

enlarged view of the spectrum, and the curve-fitting results, respectively. Three molecular structures of the MDP-Ca salts were identified (Table 1). In particular, the peaks marked 3, 5, and 6 in the ^{31}P NMR spectrum were assigned to DCS-MD, MCS-MM, and MCS-MD, respectively. After peak separation and area calculation, the percentages of DCS-MD, MCS-MM, and MCS-MD were calculated to be 26.5%, 33.8%, and 22.7%, respectively.

TEM Observations

The TEM images revealed the presence of highly ordered nanolayers (Figure 2A and B), crystalline species (Figure 2C), and lattice fringes (Figure 2B and C) in untreated MDP-Ca salt. The fast Fourier transform (FFT) image in Figure 2D shows an amorphous diffraction pattern. The nanolayer thickness (n = 5) estimated by inverse fast Fourier transform (IFFT) of the FFT images was 3.51 nm. The nanolayers became scarce, discontinuous, and partially deteriorated after attack by an acidic solution for 15 min (Figure 2E); no significant difference was detected upon attack with deionized water (Figure 2F).

ICP-MS

According to the ICP-MS results (Figure 3), a small number of Ca^{2+} ions were released from MDP-Ca salts. The concentration of Ca^{2+} ions grew slowly as the soaking time increased; both the concentration and rate of increase were larger in the acidic than neutral environment. The amount of Ca^{2+} ions released by the mixture of MDP and HAp in the acidic environment was much smaller than that released by untreated HAp.

MD Simulations

As shown in Figure 4A, Ca^{2+} ions and MDP were produced by MSC-MD after hydrolysis in an acidic environment. The structure then started to collapse dramatically after 50 ps. At the same time, Ca^{2+} ions continued to bind with the phosphate group of MDP. Free Ca^{2+} ions appeared in the solution at 500 ps, and MDP molecules aggregated in clusters. Additional Ca^{2+} ions were released in the solution after 5 ns, and the MDP molecules formed large clusters. The clusters remained stable in the following simulation, and all Ca^{2+} ions separated from the MDP molecule to interact with water molecules in the aqueous solution. In contrast to the acidic environment, Figure 4B shows that MDP and OH^- ions were formed after hydrolysis in a neutral environment. In the latter, Ca^{2+} ions always interacted with the phosphate group,

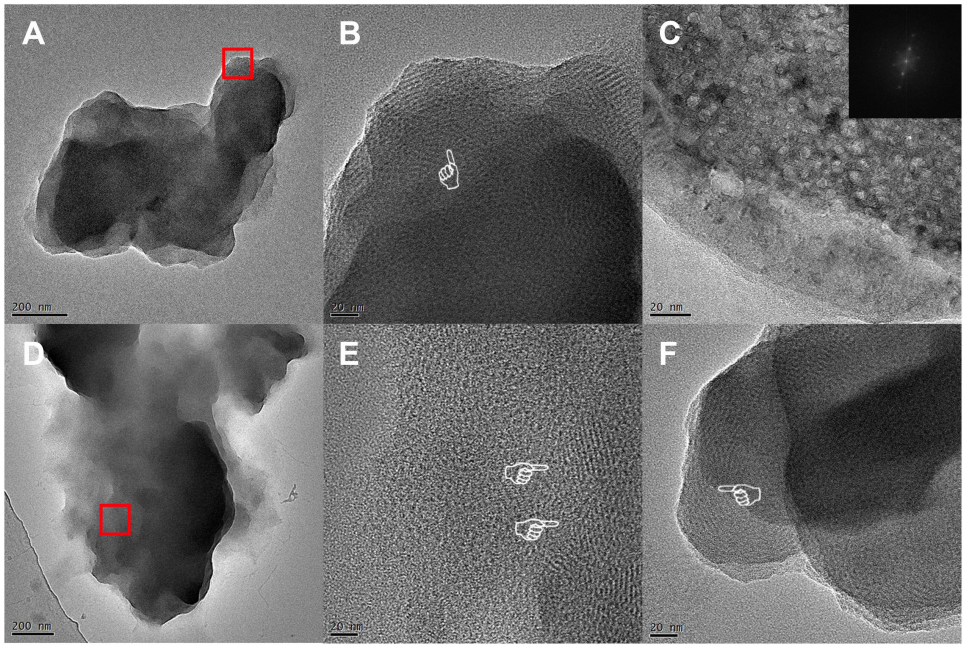

Figure 2 TEM results. (**A**) TEM image of untreated MDP-Ca salt. (**B**) Formation of nanolayered structure on untreated MDP-Ca salt, as observed by TEM. (**C**) TEM image of crystallites within untreated MDP-Ca salt and corresponding diffraction pattern obtained by FFT. (**D**) TEM image of MDP-Ca salt by attack with acidic solution for 15 min. (**E**) Discontinuous nanolayered structure of MDP-Ca salt by attack with acidic solution for 15 min. (**F**) Nanolayered structure of MDP-Ca salt by attack with neutral solution for 15 min.

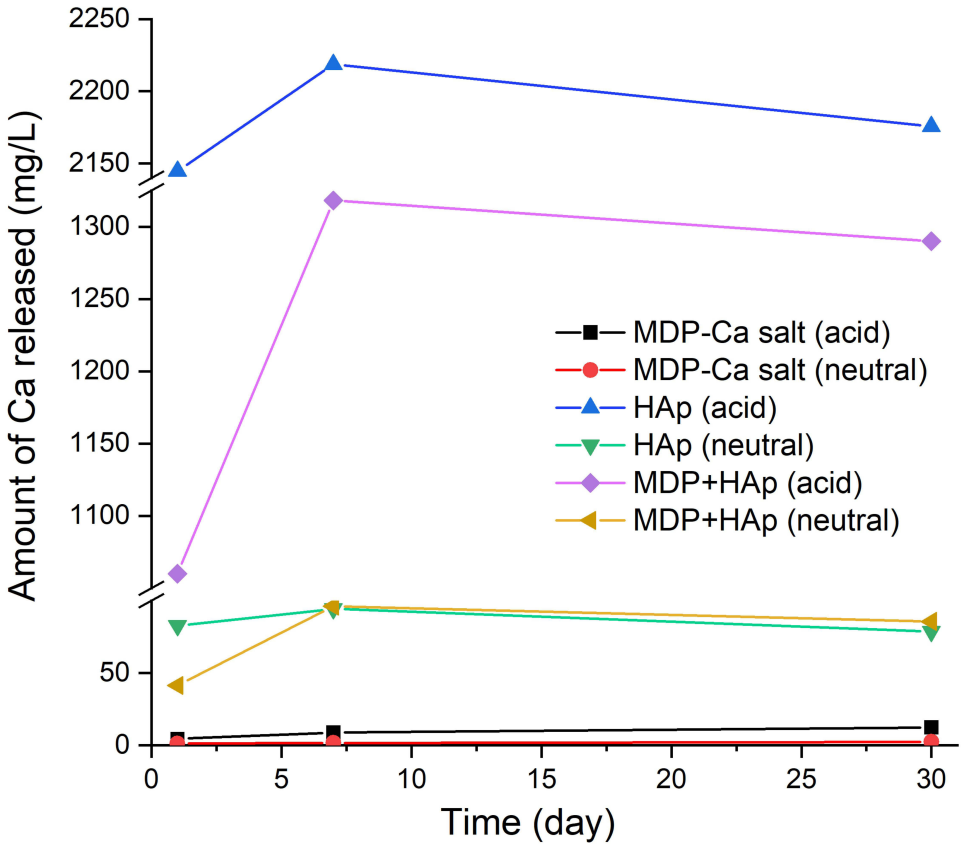

Figure 3 Calcium release from MDP-Ca salts in acid and neutral environments, as measured by ICP-MS.

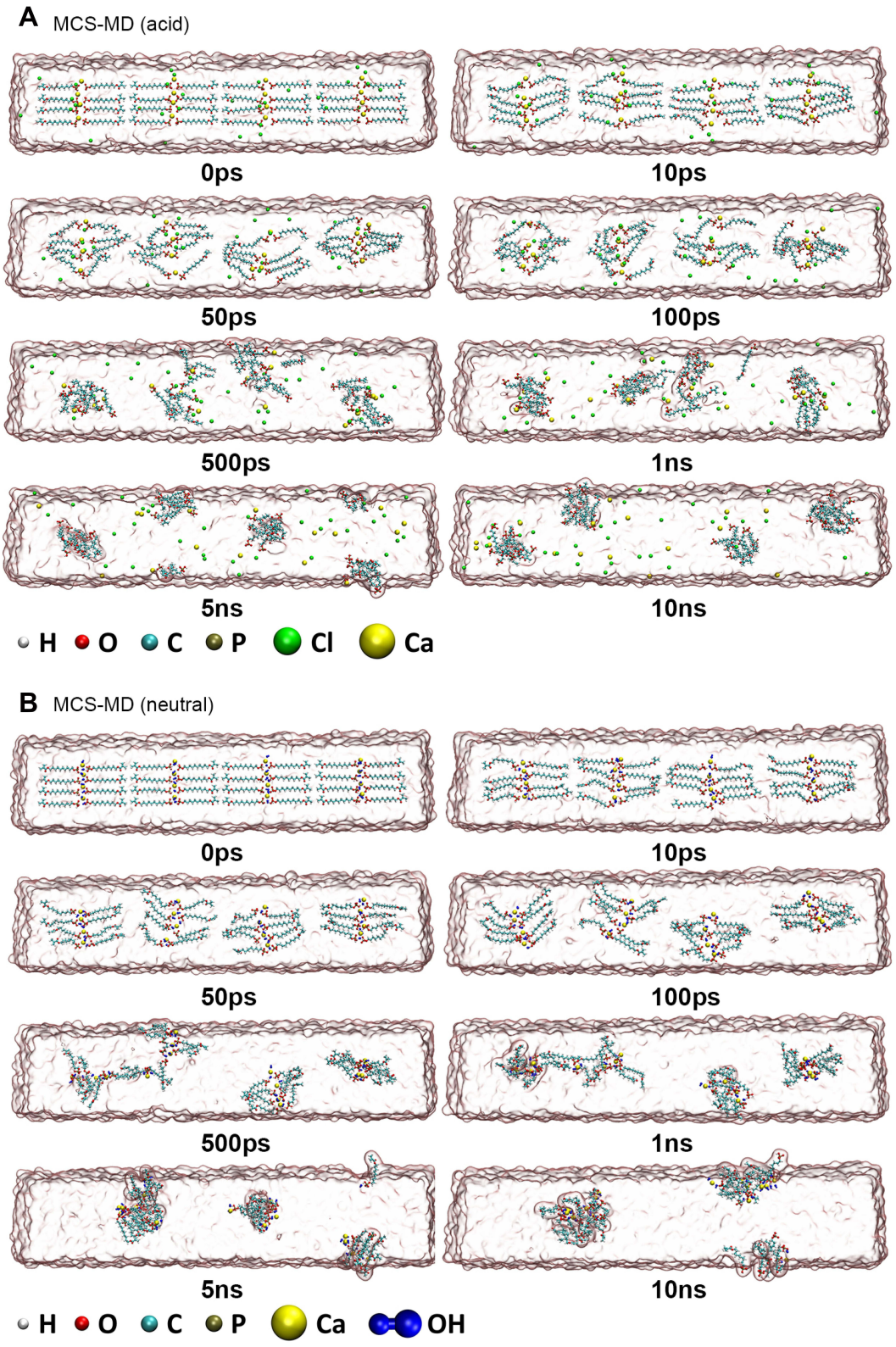

Figure 4 Evolution of MCS-MD hydrolysis in acidic and neutral environments. (**A**) MD models of MCS-MD molecules in the acidic environment. Yellow and green spheres represent Ca^{2+} and Cl^{-} ions, respectively. The nanolayered structure loose with free Ca^{2+} ions and MDP molecules form clusters. (**B**) MD models of MCS-MD molecules in the neutral environment. Connected blue spheres represent OH^{-} ions. Ca^{2+} ions always interact with the phosphate group, OH^{-} ions, and water molecules to form cluster structures with a Ca^{2+} core.

OH^- ions, and water molecules, forming cluster structures with a core consisting of Ca^{2+} ions, which remained stable for 10 ns.

After 50 ps in the acidic environment, the nanolayered structures collapsed, accompanied by the dispersion of Ca^{2+} ions and the aggregation of MDP molecules, as illustrated in Figure 5A. Ca^{2+} ions became evenly distributed in the aqueous solution with increasing time, forming coordination structures with water, while MDP molecules formed aggregates of various sizes. The structure evolved in the same way as MCS-MD in neutral conditions, with two OH^- around each Ca^{2+} ion, forming an initial coordination layer with water molecules and the oxygen atoms of the phosphoric acid group. As illustrated in Figure 5B, the final formed cluster was a large structure consisting of aggregated Ca^{2+}, OH^-, and MDP species, with no ions released into the aqueous solution.

The interaction of MDP, OH^-, and Ca^{2+} ions formed monomers of the amorphous MCS-MM, which randomly distributed in the aqueous solution rather than forming nanolayers (Figure 6A). These monomers began to assemble after 100 ps of the simulation in the acidic environment, and Ca^{2+} ions started to scatter in the aqueous solution. Finally, the process of cluster formation was the same as that of the nanolayers. $Ca(OH)_2$ was generated following hydrolysis in the neutral environment and continued to interact with water molecules and oxygen atoms of the phosphoric acid group, eventually forming clusters of various sizes (Figure 6B).

Figure 7 shows the coordination numbers of Ca^{2+} ions during the simulation; considerable differences in coordination numbers were observed between the acidic and neutral environments. Because the Ca^{2+} ions were free after hydrolysis in the acidic environment and eventually coordinated water molecules in aqueous solution, the average coordination number remained almost unchanged and fluctuated around 8 throughout the simulation. The coordination number was lower in the neutral than in the acidic environment. In particular, the average coordination number for DCS-MD was around 5, which was lower than the coordination number (7) obtained for both MCD-MD and MCS-MM. Figure 8 shows the total, Coulomb, and van der Waals energies of MCS-MD, DCS-MD and MCS-MM during the simulations in acidic and neutral environments. In both systems, the energies showed no significant changes as the simulation time increased.

Discussion

MDP-Ca salts produced by the reaction of MDP-based primers and adhesives and tooth enamel can be detected via analytical chemistry techniques and electron microscopy observation. However, their amount is not sufficient for further treatment and analysis. Although a large amount of MDP-Ca salts is produced by mixing HAp and MDP-based primers, the reaction products [HAp and dicalcium phosphate dihydrate (DCPD)] may affect the chemical characterization; this problem remains unresolved.[32] Therefore, in the present study we exploited the chemical interaction between $CaCl_2$ and MDP to produce MDP-Ca salts without coexisting HAp or amorphous DCPD.[22,33] The production ratio of each MDP-Ca salt can be tuned by changing the molar ratio of $CaCl_2$ to MDP.[33] A $CaCl_2$/MDP molar ratio of 1:1 was selected to mimic the typical ratios of MDP-Ca salts formed by natural tooth hard tissues.

The three characteristic peaks in the XRD pattern of Figure 1A, attributed to the crystalline phase generated by the layered structures, reflect the mesoporosity produced by highly ordered, porous amorphous solids.[32] After the hydroxyl group linked to the phosphate group reacts with Ca^{2+} ions, the chemical shift of the ^{31}P NMR peak depends on the environment surrounding the phosphorus atom.[33] These characterization techniques help to evaluate the molecular species and amount of MDP-Ca salts produced in the reactant.[34]

The formation of a nanolayered structure with constant spacing was clearly visible in the high-resolution TEM (HRTEM) images. The *d*-spacing calculated from the XRD pattern was 3.84 nm, similar to the nanolayer thickness measured by IFFT. A much higher content of crystalline species with amorphous structures than regular nanolayer structures was observed in the TEM images, as confirmed by the analysis of lattice fringes and FFT diffraction patterns.[35,36] This component mostly consisted of amorphous MCS-MM, in agreement with an earlier study.[22] The reactions of $CaCl_2$ with MDP to form MDP-Ca salts are as follows:

$$R-O-OP(OH)_2+Ca^{2+}+H_2O \rightarrow R-O-OP(OH)-O-CaOH+2H^+ \quad (1)$$

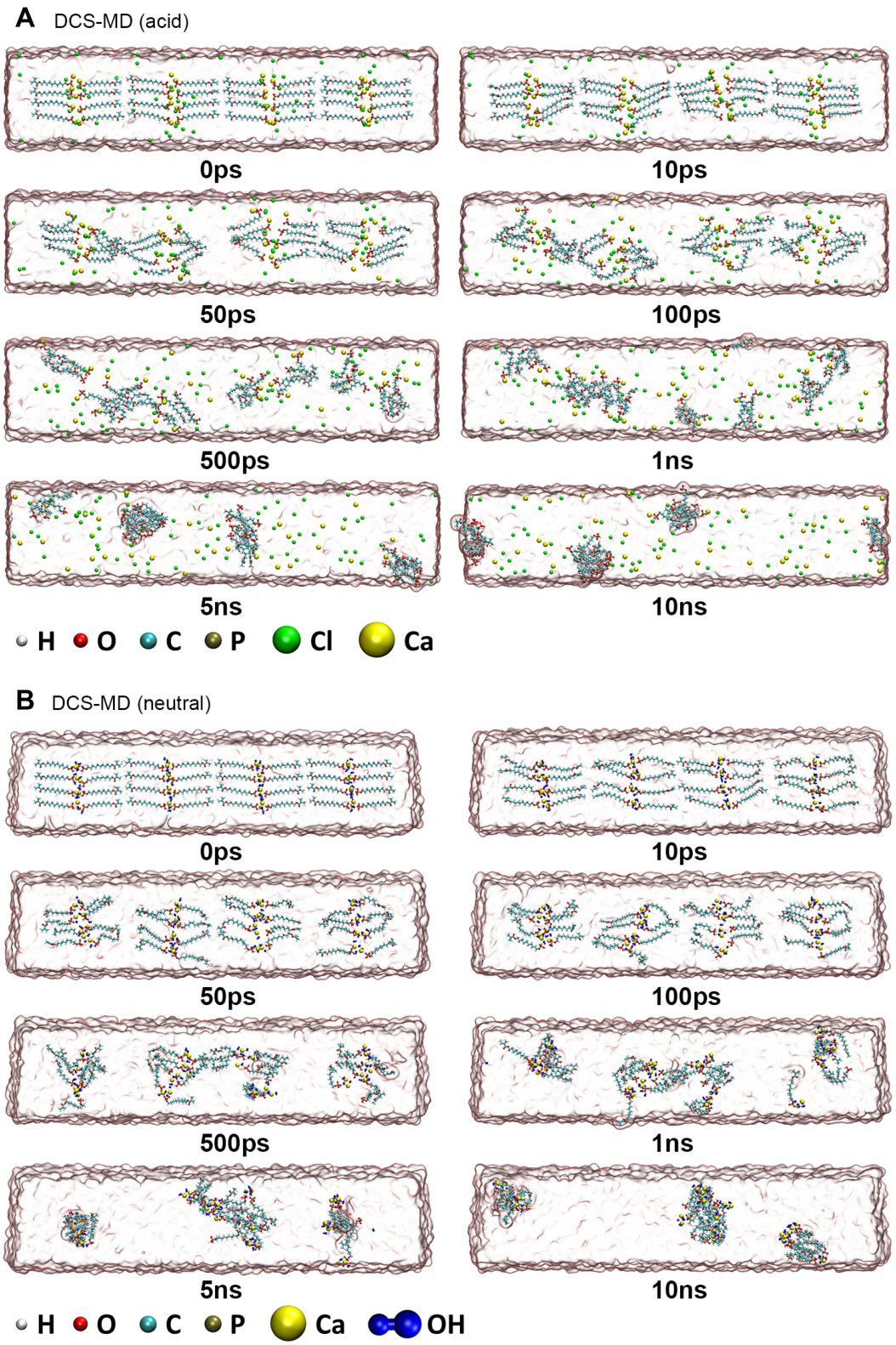

Figure 5 Evolution of DCS-MD hydrolysis in acidic and neutral environments. (**A**) MD models of DCS-MD molecules in the acidic environment. Yellow and green spheres represent Ca^{2+} and Cl^{-} ions, respectively. The nanolayered structure collapses in the acidic environment, along with the release of Ca^{2+} ions and the aggregation of MDP molecules. As the hydrolysis proceeds, MDP molecules form aggregates of different sizes. (**B**) MD models of DCS-MD molecules in the neutral environment. Connected blue spheres represent OH^{-} ions. In the neutral environment, the structure evolves into a system with two OH^{-} around each Ca^{2+} ion, forming the first coordination layer with water molecules and the oxygen atoms of the phosphoric acid group. The final formed cluster is a large aggregate of Ca^{2+}, OH^{-}, and MDP molecules.

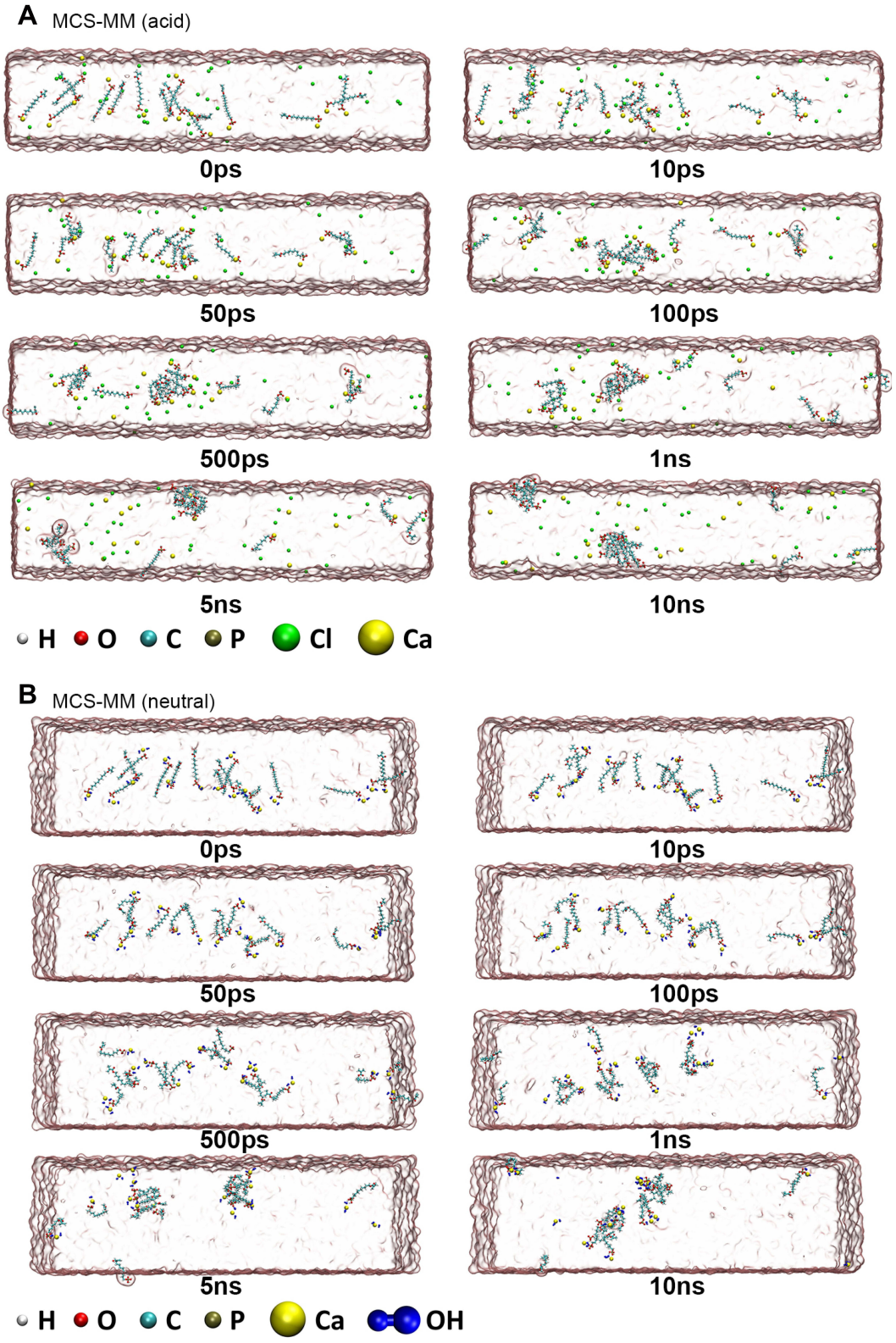

Figure 6 Evolution of MCS-MM hydrolysis in acidic and neutral environments. (**A**) MD models of amorphous MCS-MM molecules in the acidic environment. MCS-MM was randomly distributed in rectangular water boxes. Yellow and green spheres represent Ca^{2+} and Cl^{-} ions, respectively. In the acidic environment, Ca^{2+} ions dissolve in the aqueous solution and MDP molecules aggregate to form clusters. (**B**) MD models of MCS-MM molecules in the neutral environment. Connected blue spheres represent OH^{-} ions. In the neutral environment, $Ca(OH)_2$ is formed after hydrolysis and continues to interact with water molecules and oxygen atoms of the phosphoric acid group, eventually forming clusters of various sizes.

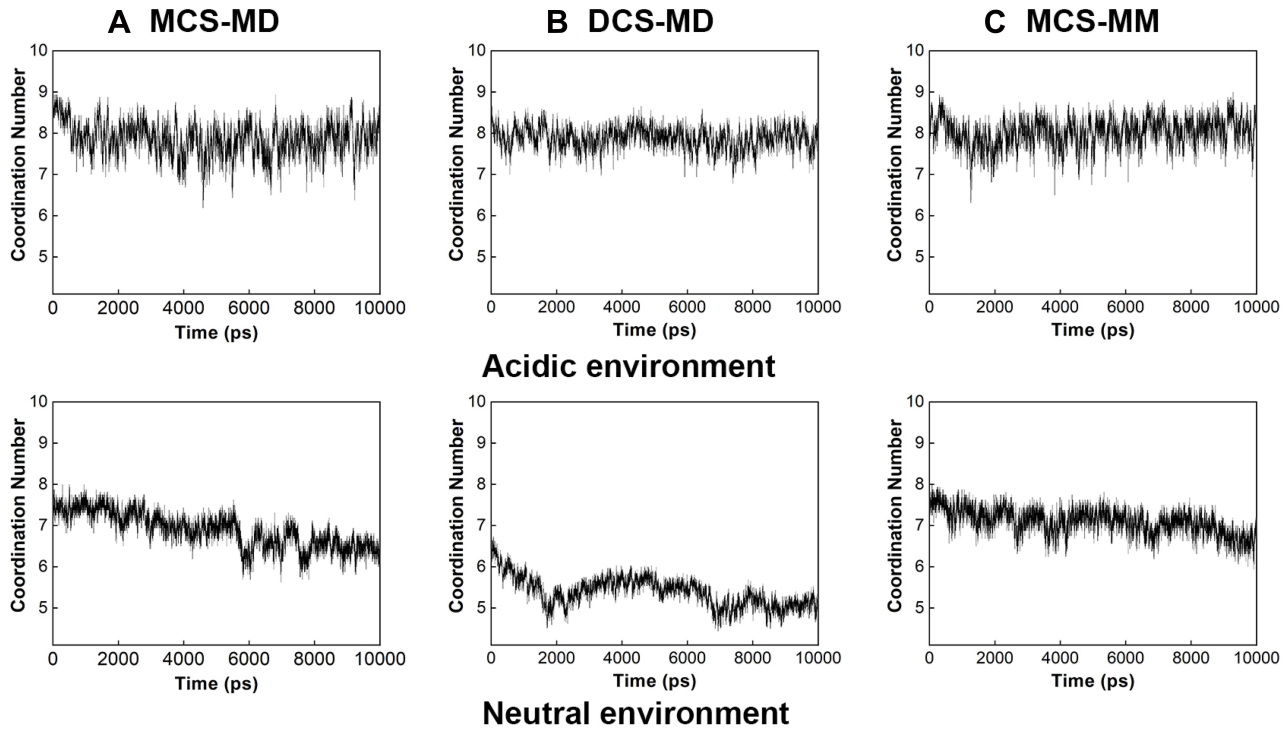

Figure 7 Coordination number of Ca^{2+} ions during simulations of (**A**) MCS-MD, (**B**) DCS-MD, and (**C**) MCS-MM in acidic and neutral environments (Ca–O bond length < 3.0 Å).

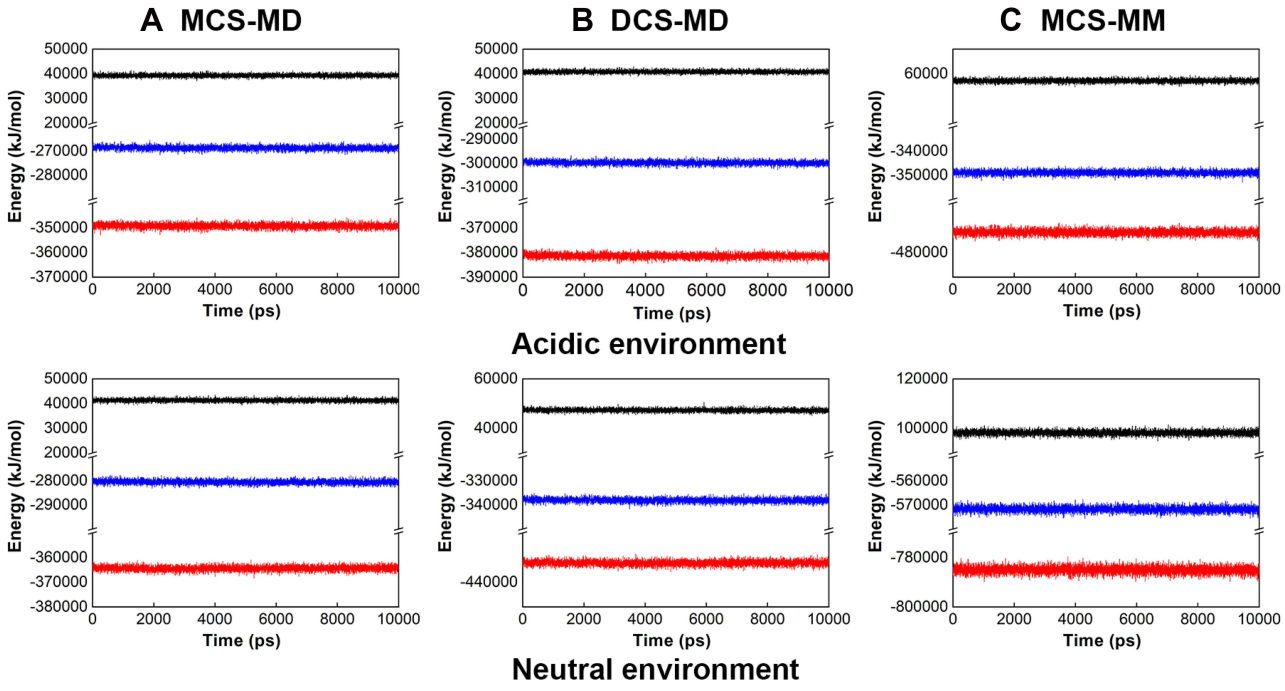

Figure 8 Time evolution of total (blue), Coulomb (red), and van der Waals (black) energies of (**A**) MCS-MD, (**B**) DCS-MD, and (**C**) MCS-MM in acidic and neutral environments.

$$2R-O-OP(OH)_2+2Ca^{2+}\rightarrow R-O-OP-(OCaO)_2-OP-O-R+4H^+ \quad (2)$$

$$2R-O-OP(OH)_2+Ca^{2+}\rightarrow R-O-OP(OH)-OCaO-OP(OH)-O-R+2H^+ \quad (3)$$

$$R=CH_2C(CH_3)COO(CH_3)_{10}$$

Based on these equations, the synthesized MDP-Ca salts undergo hydrolysis under acidic conditions, corresponding to the inverse of the above reactions. According to the ideal state modeled in the MD simulations, Ca^{2+} ions are not free in the water solution in neutral conditions, but they combine with phosphate groups, OH^- ions, and water molecules to form cluster structures with a Ca^{2+} core. However, in real systems Ca^{2+} ions are partially free in a neutral aqueous solution, and their concentration is higher in an acidic environment. As a result, it can be inferred that MDP-Ca salts are more prone to hydrolyze in the acidic environment. HRTEM images showed that the the nanolayer structure became disrupted and discontinuous upon acid attack. ICP-MS was used to verify the validity of the MD analysis by investigating the hydrolysis of the MDP-Ca salts under acidic and neutral conditions. In combination with the HRTEM findings, the results showed that the pH had a limited effect on the collapse of the nanolayered structure and breakdown of ionic bonds in MDP-Ca salts, and the MDP-Ca salts maintained a relatively stable structure in the acidic environment. Based on these observations, the first hypothesis that the hydrolytic degradation rate of MDP-Ca salts is affected by the pH environments can be accepted.

In this study, HAp and the MDP/HAp mixture were used as control. Even though dentin powder would be closer to clinical conditions, we selected HAp because other components of dentin, such as calcium carbonate, interfere with the quantification of the calcium release.[37,38] The ICP-MS results revealed that HAp rapidly released a large number of Ca^{2+} ions in an acidic environment; then, the release rate gradually leveled off. However, the amount of free Ca^{2+} ions was sharply reduced after treatment with the MDP-containing primer. This was attributed to the fact that the stable MDP-Ca salts on the surface of HAp reduced the exposed surface area, while the solubility of calcium salts is much lower than that of HAp. In the oral cavity, dentin is constantly in contact with body fluids such as blood serum and saliva.[39] A highly-ordered bound water layer covers the surface of Hap, providing an efficient proton pool for ions and chemical groups;[14] therefore, the dissolution of HAp is unavoidable. The adsorption of MDP-Ca salts on the HAp surface is similar to the modification of the same surface.[15] The high hydrophobicity of the nanolayered structure of MCS-MD and DCS-MD protects the hybrid layer from degradation, not only by directly preserving collagen fibrils from water-induced degradation, but also by improving the resistance to acidic dissolution of the remaining HAp.[6] The above advantages are reflected in the presence of MDP-Ca salts and nanolayers at the adhesive–dentin interface. Recent investigations have assessed whether the thin nanolayer can contribute to the durability of the resin–dentin bond in clinical cases,[14,32] but no studies have focused on the abundant MCS-MM component without layered structure. Compared to solid crystal structures, the high-energy amorphous MCS-MM has a higher solubility.[40] The solubility product constant (k_{sp}) of the salt species and the pH of the aqueous environment control the deposition of MDP-Ca salts.[14] The MCS-MM state on the dentin bonding interface needs further investigation. MDP-Ca salts were embedded in a thin hybrid layer after the application of self-etching adhesives. According to the above data, the exceptionally low solubility of MDP-Ca salts strengthens the hybrid layer.[41]

To further investigate the resistance of different types of MDP-Ca salts to acidic environments, the first step is to separate these salts. However, the separation of multiple forms of synthetic or natural MDP-Ca salts is an almost impossible task, except in MD-simulated solutions. MD is a useful tool for understanding complex mechanisms, discovering new phenomena, quantitatively simulating processes, and calculating the affinities of small molecules to binding sites.[42,43] At 500 ps for MCS-MD, 50 ps for DCS-MD, and 100 ps for MCS-MM, the Ca^{2+} ions began to drift away into the aqueous solution; the above times were calculated as the time points when a Ca^{2+} ion separated from the phosphoric acid of MDP. The reason for the different dissociation times could be that, in the hydrolysis process, two phosphate groups of MCS-MD interact with a Ca^{2+} ion, whereas DCS-MD has two phosphate groups interacting with two Ca^{2+} ions; this results in a stronger electrostatic attraction in the case of MCS-MD, with a corresponding lower

release of Ca^{2+} ions into the aqueous solution. After hydrolysis, only one phosphoric acid group interacts with a Ca^{2+} ion in amorphous MCS-MM, resulting in the time of the first release of the Ca^{2+} ion in acidic environments to be between those of MCS-MD and DCS-MD. The layered MDP molecules improve the stability of the nanolayer, owing to the polymerization of adjacent C=C bonds.[14] The mechanical properties of the nanolayer are intermediate between those of the adhesive and the resin; the nanolayer grows into the hybrid layer and extends to the interface between the them, which enhances the functional gradient at the adhesive–dentin interface.[17] Amorphous MDP-Ca salt is deposited in both the hybrid layer and the adhesive, compromising the durability of the resin–dentin bond. As shown by the ICP-MS results, in an acidic environment the ionic bonds in the layered MDP-Ca salts and the amorphous phase break with time, resulting in the gradual hydrolysis of the salts. Based on these findings, the second hypothesis that the nanolayered structure of the MDP-Ca salt provides better resistance to acid degradation than the amorphous form should be rejected.

Conclusion

Within the limitations of this study, the following conclusions can be drawn based on the reported findings:

In acidic conditions, the hydrolysis of MDP-Ca salts can proceed at a faster rate than in neutral environments; MCS-MD with nanolayered structure has the highest resistance to acidic hydrolysis, followed by amorphous MCS-MM and DCS-MD. The nanolayers are destroyed by the acidic environment, whereas MDP-Ca salts in the layered or amorphous structures are slowly hydrolyzed.

Acknowledgments

This work was supported by the National Natural Science Foundation of China [grant 81970927]; the Natural Science Foundation of Jiangsu Province of China [BK20191348]; the Qing Lan Project and the Priority Academic Program Development of Jiangsu Higher Education Institutions [grant 2018-87].

Disclosure

The authors report no conflicts of interest in this work.

References

1. Frassetto A, Breschi L, Turco G, et al. Mechanisms of degradation of the hybrid layer in adhesive dentistry and therapeutic agents to improve bond durability–A literature review. *Dent Mater*. 2016;32(2):e41–53. doi:10.1016/j.dental.2015.11.007
2. Pereira JR, Pamato S, Vargas M, Junior NF. State of the art of dental adhesive systems. *Curr Drug Deliv*. 2018;15(5):610–619. doi:10.2174/1567201814666171120120935
3. Peng W, Yi L, Wang Z, Yang H, Huang C. Effects of resveratrol/ethanol pretreatment on dentin bonding durability. *Mater Sci Eng C Mater Biol Appl*. 2020;114:111000. doi:10.1016/j.msec.2020.111000
4. Nagarkar S, Theis-Mahon N, Perdigão J. Universal dental adhesives: current status, laboratory testing, and clinical performance. *J Biomed Mater Res B Appl Biomater*. 2019;107(6):2121–2131. doi:10.1002/jbm.b.34305
5. Shen J, Xie H, Wang Q, Wu X, Yang J, Chen C. Evaluation of the interaction of chlorhexidine and MDP and its effects on the durability of dentin bonding. *Dent Mater*. 2020;36(12):1624–1634. doi:10.1016/j.dental.2020.10.006
6. Yoshihara K, Yoshida Y, Nagaoka N, et al. Nano-controlled molecular interaction at adhesive interfaces for hard tissue reconstruction. *Acta Biomater*. 2010;6(9):3573–3582. doi:10.1016/j.actbio.2010.03.024
7. Kanzow P, Krois J, Wiegand A, Schwendicke F. Long-term treatment costs and cost-effectiveness of restoration repair versus replacement. *Dent Mater*. 2021;37(6):e375–e381. doi:10.1016/j.dental.2021.02.008
8. Kanzow P, Wiegand A, Schwendicke F. Cost-effectiveness of repairing versus replacing composite or amalgam restorations. *J Dent*. 2016;54:41–47. doi:10.1016/j.jdent.2016.08.008
9. Dressano D, Salvador MV, Oliveira MT, et al. Chemistry of novel and contemporary resin-based dental adhesives. *J Mech Behav Biomed Mater*. 2020;110:103875. doi:10.1016/j.jmbbm.2020.103875
10. Awad MM, Alhalabi F, Alshehri A, et al. Effect of non-thermal atmospheric plasma on micro-tensile bond strength at adhesive/dentin interface: a systematic review. *Materials*. 2021;14(4):1026. doi:10.3390/ma14041026
11. Yoshida Y, Nagakane K, Fukuda R, et al. Comparative study on adhesive performance of functional monomers. *J Dent Res*. 2004;83(6):454–458. doi:10.1177/154405910408300604
12. Van Landuyt KL, Kanumilli P, De Munck J, Peumans M, Lambrechts P, Van Meerbeek B. Bond strength of a mild self-etch adhesive with and without prior acid-etching. *J Dent*. 2006;34(1):77–85. doi:10.1016/j.jdent.2005.04.001
13. Zhou J, Wurihan SY, Tanaka R, et al. Quantitative/qualitative analysis of adhesive-dentin interface in the presence of 10-methacryloyloxydecyl dihydrogen phosphate. *J Mech Behav Biomed Mater*. 2019;92:71–78. doi:10.1016/j.jmbbm.2018.12.038
14. Tian FC, Wang XY, Huang Q, et al. Effect of nanolayering of calcium salts of phosphoric acid ester monomers on the durability of resin-dentin bonds. *Acta Biomater*. 2016;38:190–200. doi:10.1016/j.actbio.2016.04.034

15. Fukegawa D, Hayakawa S, Yoshida Y, Suzuki K, Osaka A, Van Meerbeek B. Chemical interaction of phosphoric acid ester with hydroxyapatite. *J Dent Res*. 2006;85(10):941–944. doi:10.1177/154405910608501014
16. Yoshida Y, Yoshihara K, Nagaoka N, et al. Self-assembled Nano-layering at the Adhesive interface. *J Dent Res*. 2012;91(4):376–381. doi:10.1177/0022034512437375
17. Yoshihara K, Nagaoka N, Nakamura A, Hara T, Yoshida Y, Van Meerbeek B. Nano-layering adds strength to the adhesive interface. *J Dent Res*. 2021;100(5):515–521. doi:10.1177/0022034520979133
18. Yoshihara K, Nagaoka N, Yoshida Y, Van Meerbeek B, Hayakawa S. Atomic level observation and structural analysis of phosphoric-acid ester interaction at dentin. *Acta Biomater*. 2019;97:544–556. doi:10.1016/j.actbio.2019.08.029
19. Breschi L, Mazzoni A, Ruggeri A, et al. Dental adhesion review: aging and stability of the bonded interface. *Dent Mater*. 2008;24(1):90–101. doi:10.1016/j.dental.2007.02.009
20. Sarr M, Kane AW, Vreven J, et al. Microtensile bond strength and interfacial characterization of 11 contemporary adhesives bonded to bur-cut dentin. *Oper Dent*. 2010;35(1):94–104. doi:10.2341/09-076-L
21. Peumans M, De Munck J, Van Landuyt K, Van Meerbeek B. Thirteen-year randomized controlled clinical trial of a two-step self-etch adhesive in non-carious cervical lesions. *Dent Mater*. 2015;31(3):308–314. doi:10.1016/j.dental.2015.01.005
22. Yaguchi T. Layering mechanism of MDP-Ca salt produced in demineralization of enamel and dentin apatite. *Dent Mater*. 2017;33(1):23–32. doi:10.1016/j.dental.2016.09.037
23. Zhang L, Wang W, Wang C, et al. Interaction of ACP and MDP and its effect on dentin bonding performance. *J Mech Behav Biomed Mater*. 2019;91:301–308. doi:10.1016/j.jmbbm.2018.12.017
24. Sansone C, Van Houte J, Joshipura K, Kent R, Margolis HC. The association of mutans streptococci and non-mutans streptococci capable of acidogenesis at a low pH with dental caries on enamel and root surfaces. *J Dent Res*. 1993;72(2):508–516. doi:10.1177/00220345930720020701
25. Bowen WH, Burne RA, Wu H, Koo KH. Oral biofilms: pathogens, matrix, and polymicrobial interactions in microenvironments. *Trends Microbiol*. 2018;26(3):229–242. doi:10.1016/j.tim.2017.09.008
26. Melo ESP, Melo E, Arakaki D, Michels F, Nascimento VA. Methodology to quantify and screen the demineralization of teeth by immersing them in acidic drinks (Orange Juice, Coca-Cola™, and Grape Juice): evaluation by ICP OES. *Molecules*. 2021;26(11):3337. doi:10.3390/molecules26113337
27. Van Der Spoel D, Lindahl E, Hess B, et al. GROMACS: fast, flexible, and free. *J Comput Chem*. 2005;26(16):1701. doi:10.1002/jcc.20291
28. Frisch MJ, Trucks GW, Schlegel HB, et al. *Gaussian 16, Revision A.03*. Wallingford, CT, USA: Gaussian; 2016.
29. Wang JM, Cieplak P, Kollman PA. How well does a restrained electrostatic potential (RESP) model perform in calculating conformational energies of organic and biological molecules? *J Comput Chem*. 2000;21(12):1049–1074. doi:10.1002/1096-987X(200009)21:12<1049::AID-JCC3>3.0.CO;2-F
30. Wang J, Wang W, Kollman PA, Case DA. Automatic atom type and bond type perception in molecular mechanical calculations. *J Mol Graph Model*. 2006;25(2):247260. doi:10.1016/j.jmgm.2005.12.005
31. Darden T, York D, Pedersen L. Particle mesh Ewald: an Nlog(N) method for Ewald sums in large systems. *J Chem Phys*. 1993;98(12):10089. doi:10.1063/1.464397
32. Tian F, Zhou L, Zhang Z, et al. Paucity of nanolayering in resin-dentin interfaces of MDP-based adhesives. *J Dent Res*. 2016;95(4):380–387. doi:10.1177/0022034515623741
33. Yokota Y, Nishiyama N. Determination of molecular species of calcium salts of MDP produced through decalcification of enamel and dentin by MDP-based one-step adhesive. *Dent Mater J*. 2015;34(2):270–279. doi:10.4012/dmj.2014-260
34. Fujita Nakajima K, Nikaido T, Arita A, Hirayama S, Nishiyama N. Demineralization capacity of commercial 10-methacryloyloxydecyl dihydrogen phosphate-based all-in-one adhesive. *Dent Mater*. 2018;34(10):1555–1565. doi:10.1016/j.dental.2018.06.027
35. Jokisaari JR, Wang C, Qiao Q, et al. Particle-attachment-mediated and Matrix/Lattice-guided enamel apatite crystal growth. *ACS Nano*. 2019;13(3):3151–3161. doi:10.1021/acsnano.8b08668
36. Bachmatiuk A, Zhao J, Gorantla SM, et al. Low voltage transmission electron microscopy of graphene. *Small*. 2015;11(5):515–542. doi:10.1002/smll.201401804
37. Yoshihara K, Hayakawa S, Nagaoka N, Okihara T, Yoshida Y, Van Meerbeek B. Etching efficacy of self-etching functional monomers. *J Dent Res*. 2018;97(9):1010–1016. doi:10.1177/0022034518763606
38. Porębska A, Różycka M, Hołubowicz R, Szewczuk Z, Ożyhar A, Dobryszycki P. Functional derivatives of human dentin matrix protein 1 modulate morphology of calcium carbonate crystals. *FASEB J*. 2020;34(5):6147–6165. doi:10.1096/fj.201901999R
39. Bertazzo S, Zambuzzi WF, Campos DD, Ogeda TL, Ferreira CV, Bertran CA. Hydroxyapatite surface solubility and effect on cell adhesion. *Colloids Surf B Biointerfaces*. 2010;78(2):177–184. doi:10.1016/j.colsurfb.2010.02.027
40. Shi Q, Li F, Yeh S, Wang Y, Xin J. Physical stability of amorphous pharmaceutical solids: nucleation, crystal growth, phase separation and effects of the polymers. *Int J Pharm*. 2020;590:119925. doi:10.1016/j.ijpharm.2020.119925
41. Yoshihara K, Yoshida Y, Hayakawa S, et al. Self-etch monomer-calcium salt deposition on dentin. *J Dent Res*. 2011;90(5):602–606. doi:10.1177/0022034510397197
42. Asakura T. Structure and dynamics of spider silk studied with solid-state nuclear magnetic resonance and molecular dynamics simulation. *Molecules*. 2020;25(11):2634. doi:10.3390/molecules25112634
43. Al-Khafaji K, Taskin Tok T. Molecular dynamics simulation, free energy landscape and binding free energy computations in exploration the anti-invasive activity of amygdalin against metastasis. *Comput Methods Programs Biomed*. 2020;195:105660. doi:10.1016/j.cmpb.2020.105660